ONLINE SUPPLEMENT

PPARγ Level Contributes to Structural Integrity and Component Production of Elastic Fibers in the Aorta

Haw-Chih Tai, MS[1,2]; Pei-Jane Tsai, PhD[3]; Ju-Yi Chen, MD, PhD[1,2,4]; Chao-Han Lai, MD, PhD[1,2,5]; Kuan-Chieh Wang, PhD[2,6]; Shih-Hua Teng, PhD[7]; Shih-Chieh Lin, PhD[8]; Alice Y.W. Chang[8]; Meei-Jyh Jiang, PhD[2,9]; Yi-Heng Li, MD, PhD [2,4]; Hua-Lin Wu, PhD[2,6]; Nobuyo Maeda, PhD[10]; and Yau-Sheng Tsai, PhD[1,2,11]

[1]Institute of Clinical Medicine, [2]Cardiovascular Research Center, [3]Department of Medical Laboratory Science and Biotechnology, [6]Department of Biochemistry and Molecular Biology, [8]Department of Physiology, and [9]Department of Cell Biology and Anatomy, National Cheng Kung University, Tainan, Taiwan, ROC; [4]Department of Internal Medicine, [5]Department of Surgery, and [11]Research Center of Clinical Medicine, National Cheng Kung University Hospital, College of Medicine, National Cheng Kung University, Tainan, Taiwan, ROC; [7]Graduate Institute of Biomedical Sciences, Chang Gung University, Taoyuan, Taiwan, ROC; [10]Department of Pathology and Laboratory Medicine, University of North Carolina at Chapel Hill, Chapel Hill, NC, USA

Address Correspondence to:

Yau-Sheng Tsai, 1 University Road, National Cheng Kung University, Tainan 701, Taiwan. Phone: 886-6-2353535-4242; Fax: 886-6-2758781; E-mail: yaustsai@mail.ncku.edu.tw

Supplemental Methods

Mice

Generation of mice carrying the modified *Pparg* locus has been described.[1] $Pparg^{C/C}$, $Pparg^{C/+}$, and $Pparg^{+/+}$ mice were littermates of F2 generation from a cross between 129S6 and C57BL/6J F1 heterozygotes. The *Pparg*-C allele was subsequently placed on a C57BL/6J background by backcrossing for eight generations. $Pparg^{+/+}$, $Pparg^{+/-}$ and $Pparg^{C/-}$ mice were F1 littermates from the mating of $Pparg^{C/+}$ mice on a C57BL/6J background with $Pparg^{+/-}$ mice on a 129S6 background (kindly provided by Dr. Ronald Evans at the Salk Institute).[2] For AngII infusion, anesthetized mice received subcutaneous implantation of ALZET osmotic minipumps (1004; DURECT Corporation), delivering AngII (A9525; Sigma-Aldrich) at 500 or 1000 ng/min/kg for 4 weeks. All AngII-infused mice were fed a western diet (D12079B; Research Diets). Doxycycline hyclate (D9891; Sigma-Aldrich) was administrated in drinking water, covered with aluminum foil, at a dose of 30 mg/kg/day and prepared fresh every other day. Mice were anesthetized by intraperitoneal injection of Zoletil-Rompun mixture (1 ml Zoletil® (50mg/ml) + 0.1ml Rompun® + 3.9 ml normal saline)，0.1 ml mixture per 20 g mouse body weight. Mice were housed in a specific pathogen-free barrier facility with the humidity and temperature controlled. All animal studies were performed according to protocols approved by the Institutional Animal Care and Use Committee of National Cheng Kung University.

Measurements of Blood Pressure

Blood pressure was measured in conscious mice by using the tail cuff blood pressure measurement system (BP-2000; Visitech Systems). The mice were training for 2 days. Blood pressures were measured 20 times per day for 3 consecutive days. The results were calculated as the average from three trials of five to ten measurements each day for 3 consecutive days. For continuous BP recording, a telemetric device (PA-C20; Data Sciences International) was implanted via the left carotid artery into the aorta. Continuous BP results were recorded every 5 minutes for 14 days beginning 10 days after surgery to allow mice to recover normal diurnal rhythms.

Immunohistochemical Staining

Paraffin-embedded sections (5 μm) were deparaffinized and rehydrated. Antigen retrieval was conducted by boiling sections in 10 mmol/L sodium citrate buffer at pH 6.0 for 10 min. Sections were incubated with primary antibodies against PPARγ (sc-7196; Santa Cruz Biotechnology), MMP-9 (AB19016; Millipore), SMactin (A2547; Sigma-Aldrich), FAP (ab53066; Abcam), MOMA-1 (GTX42355; GeneTex), CD68 (M081401; Dako) and Ki-67 (ab15580; Abcam). Secondary antibody staining (VECTASTAIN ABC kit; Vector

Laboratories) was performed. Slides were developed using 3, 3′-diaminobenzidine substrate-chromogen solution (K3468; Dako) and counterstained with hematoxylin. The specificity of PPARγ antibody was confirmed by negative control procedures, including no primary antibody control, primary antibody isotype control, and no antigen retrieval, which gave consistently negative results (Figure S1).

Consistency of Elastic Lamella

Consistency of elastic lamella was determined by the ratio of the length of elastic fibers with constant thickness to the length of the medial area section. The number of elastin breaks was counted and divided by the medial area.

RNA Analysis

Aortic tissues were stored in RNAlater (Ambion). Total RNA was extracted with REzol (Protech Technology Enterprise). Level of mRNA was analyzed with SYBR green-based real-time quantitative RT-PCR assays (StepOne; Applied Biosystems), with β-actin as the reference gene in each reaction. Sequences of the primers used for real-time PCR assays are shown in Table S5.

Immunoblot Analysis

Twenty micrograms of total proteins were subjected to electrophoresis, transferred to PVDF membranes, and probed with antibodies against tropoelastin (CL55041AP; Cedarlane), collagen type I (234167; Calbiochem), fibulin-4 (36475; Epitomics), fibulin-5 (12188-1-AP; Protein Tech), MMP-9 (AB19016; Millipore), PPARγ (2443; Cell signaling), PPARγ P-Ser112 (ab60953; Abcam), Cathepsin S (ab18822; Abcam) and α-tubulin (T5168; Sigma-Aldrich). Immunoreactive detection was performed with a chemiluminescent detection system (RPN2106; GE Healthcare).

Proteomics Analysis

The insoluble pellets of homogenized aortas (100 μg for each aorta) were used for in-solution trypsin digestion. The LC-MS/MS (HCT ultra ion trap MS; Bruker) was performed with a HPLC system (UltiMate 3000; Dionex). The sample was injected into a trap column (Acclaim PepMap100, 164199; Dionex). The trapped analyses were separated by an analytical column (Acclaim PepMap100, 164261; Dionex). Three MS only and 1 autoMSMS runs were performed for each sample. The LC-MS/MS spectra were analyzed for peptide identification by Swissport (release 56.1) database with the search engine MASCOT (version 2.2.07). The relative protein abundance based on a label free quantitative analysis was expressed as the ratio of $Pparg^{C/-}$ to $Pparg^{+/+}$ by ProteinScape 3.0 (Bruker Daltonics).

Gelatin Zymography

Aortic lysates were subjected to electrophoresis on 8% SDS-PAGE co-polymerized with 1% gelatin as the substrate. The gel was incubated at room temperature for 1 h in renaturing buffer, and incubated at 37°C for 24 h in developing buffer. The gels were stained with 0.05% Coomassie Brilliant Blue, and then destained with destain buffer.

Ultrasound Imaging

Ultrasound imaging was performed using a high-resolution ultrasound imaging system (Vevo 770; VisualSonics) with 40 MHz frequency real-time microvisualization scanhead (RMV 704). Mice were placed in a supine position on a heating pad under isoflurane anesthesia and depilated with hair removal cream. The 2D imaging in B-mode was used to localize the suprarenal abdominal aorta and the cross-sectional view was recorded to measure the diameter of aortic lumen.

Cell Culture

Human aortic smooth muscle cells (HASMCs, C-007-5C; Life Technologies) and human aortic adventitial fibroblasts (HAoAFs, CC-7014; Lonza) were derived from thoracic aorta. The culture protocols of human cells were followed the manufacturer's instructions. Rat aortic smooth muscle cells (ASMCs) and mouse embryonic fibroblasts (MEFs) were grown in DMEM containing penicillin/streptomycin supplemented with 10% FBS. Cells were treated with various stimuli for 24 hours and collected for mRNA analysis. For small interfering RNA (siRNA) knockdown, a final concentration of 40 nmol/L siRNA against PPARγ (s72013; Ambion) and scrambled control siRNA were transfected into MEFs by Lipofectamine 3000 (Life Technologies) and incubated for 3 days.

Chromatin Immunoprecipitation (ChIP) Assay

The procedure for ChIP was described previously.[3] In brief, the interaction between protein and DNA was fixed by using 1% formaldehyde for 10 minutes. Cells were harvested and sonicated to fragment DNA (average size of 200–500 bp). PPARγ antibody (ab41928; Abcam) was used to immunoprecipitate the PPARγ protein and DNA complexes. Potential PPARγ binding sites were amplified by specific primers (Table S5) after reversing cross-linking.

References

1. Tsai YS, Tsai PJ, Jiang MJ, Chou TY, Pendse A, Kim HS, Maeda N. Decreased ppar gamma expression compromises perigonadal-specific fat deposition and insulin sensitivity. *Mol Endocrinol*. 2009;23:1787-1798.
2. Barak Y, Nelson MC, Ong ES, Jones YZ, Ruiz-Lozano P, Chien KR, Koder A, Evans RM. Ppar gamma is required for placental, cardiac, and adipose tissue development. *Mol Cell*. 1999;4:585-595.
3. Lin SC, Chien CW, Lee JC, Yeh YC, Hsu KF, Lai YY, Lin SC, Tsai SJ. Suppression of dual-specificity phosphatase-2 by hypoxia increases chemoresistance and malignancy in human cancer cells. *J Clin Invest*. 2011;121:1905-1916.

Table S1. Aortic geometry of *Pparg*$^{+/+}$ and *Pparg*$^{C/-}$ mice.

Parameters	+/+ (n=5)	C/- (n=5)	*P*-value
Media thickness (μm)	44.34 ± 3.71	41.53 ± 3.71	0.67
Lumen CSA (mm^2)	0.34 ± 0.05	0.33 ± 0.06	0.89
Media CSA (mm^2)	0.09 ± 0.01	0.11 ± 0.01	0.57
Lumen / media ratio	3.31 ± 0.45	3.54 ± 0.52	0.76
Perimeter (mm)	2.54 ± 0.12	2.43 ± 0.14	0.57

CSA: cross-section area. *P*-value is resulted from Student's *t* test.

Table S2. Protein identified by a LC/MS-based label-free quantitative proteomic analysis in the insoluble fraction of aortic lysate.

Protein description	Ratio (C/- : +/+)	Quantifiable peptides	Identified peptides	Biological process
Fibulin-5	0.61	7	9	Elastic fiber assembly
Hemoglobin subunit alpha	0.71	5	7	Oxygen transport
Periostin	0.72	8	23	Extracellular matrix organization
Histone H4	0.81	3	6	DNA-binding
Cysteine and glycine-rich protein 1	0.81	3	8	Actin cytoskeleton organization
Calponin-1	0.82	4	8	Muscle contraction
Elastin	0.82	7	11	Elastic fiber assembly
Tropomyosin beta chain	0.83	4	12	Muscle contraction
Collagen alpha-2(VI) chain	0.84	8	21	Extracellular matrix organization
Fibrillin-1	0.84	7	40	Elastic fiber assembly
Decorin	0.85	3	8	Extracellular matrix organization
Hemoglobin subunit beta-1	0.87	8	13	Oxygen transport
Lysyl oxidase homolog 1	0.87	7	15	Elastic fiber assembly
Transgelin	0.89	3	14	Muscle protein
Fibronectin	0.90	12	35	Extracellular matrix organization
Prelamin-A/C	0.90	8	26	Nucleus organization
Protein-glutamine gamma-glutamyltransferase 2	0.91	4	13	G-protein coupled receptor signaling pathway
Actin, cytoplasmic 1	0.91	3	4	Actin cytoskeleton organization
Basement membrane-specific heparan sulfate proteoglycan core protein	0.92	8	37	Extracellular matrix organization
Myosin-11	0.94	36	90	Muscle contraction
Creatine kinase B-type	0.95	3	3	Cellular chloride ion homeostasis

Actin, aortic smooth muscle	0.95	15	23	Muscle contraction
Collagen alpha-1(VI) chain	0.95	4	16	Extracellular matrix organization
Myosin regulatory light polypeptide 9	0.95	3	7	Muscle contraction
ATP synthase subunit beta	0.97	4	11	ATP biosynthetic process
Filamin-A	0.99	29	81	Actin cytoskeleton organization
Vimentin	0.99	14	25	Intermediate filament organization
Tubulin alpha-1A	1.00	3	9	Microtubule organization
Collagen alpha-1(I) chain	1.00	6	8	Extracellular matrix organization
Myosin light polypeptide 6	1.01	3	7	Muscle contraction
Myosin-4	1.02	3	30	Muscle contraction
Alpha-actinin-1	1.02	10	21	Actin cytoskeleton organization
Talin-1	1.03	6	24	Actin cytoskeleton organization
ATP synthase subunit alpha	1.03	3	10	ATP biosynthetic process
Histone H2B type 3-A	1.06	3	6	DNA-binding
Collagen alpha-2(I) chain	1.09	4	7	Extracellular matrix organization
Tubulin beta-5 chain	1.17	3	8	Microtubule organization

Identified peptides: number of peptides with MASCOT individual ion score above 20. Quantifiable peptides: number of Identified peptides with quantitation ratio (C/- versus +/+). N=5 in each group.

Table S3. Aortic geometry of the mice infused with 500 ng/kg/min of AngII and fed with a western diet

Parameters		+/+ (n=5)	+/- (n=3)	C/- (n=7)	*P*-value
Medial thickness (μm)	TA	36.54 ± 0.37	33.13 ± 3.24	36.97 ± 2.39	0.55
	AA	33.36 ± 1.00	32.33 ± 1.94	32.48 ± 1.55	0.89
Elastic fiber content (arbitrary unit)	TA	1.67 ± 0.24	1.67 ± 0.17	1.36 ± 0.11	0.36
	AA	1.48 ± 0.30	0.79 ± 0.06	1.14 ± 0.23	0.29
Mean distance between elastic lamellae	TA	6.75 ± 0.21	6.25 ± 0.58	7.25 ± 0.48	0.37
	AA	7.40 ± 0.23	7.49 ± 0.68	7.26 ± 0.40	0.93
Number of elastic lamellae	TA	5.45 ± 0.20	5.31 ± 0.11	5.12 ± 0.07	0.20
	AA	4.53 ± 0.14	4.38 ± 0.15	4.48 ± 0.20	0.89

TA: thoracic aorta. AA: abdominal aorta. Elastic fiber content was quantified by the ratio of elastic fiber staining area to the medial area. Elastic fiber staining area was selected manually by a specific RGB threshold and quantified by HistoQuest software (TissueGnostics). *P*-value is resulted from one-way ANOVA analysis between three groups.

Table S4. Aortic geometry of the mice infused with 1000 ng/kg/min of AngII and fed with a western diet.

Parameters		+/+ (n=3)	C/- (n=6)
Medial thickness (μm)	TA	76.27 ± 16.99	61.78 ± 3.35
	AA	82.98 ± 17.33	55.42 ± 10.65
Elastic fiber content	TA	0.76 ± 0.07	1.10 ± 0.16
(arbitrary unit)	AA	0.92 ± 0.22	1.04 ± 0.24
Elastic fiber breaks	TA	0.56 ± 0.13	1.22 ± 0.26
(Breaks per 10000μm^2)	AA	1.06 ± 0.40	4.06 ± 1.07 *****
Mean distance between elastic lamellae	TA	13.83 ± 2.73	12.69 ± 0.90
	AA	16.57 ± 1.97	11.73 ± 2.34
Number of elastic lamellae	TA	5.51 ± 0.13	4.94 ± 0.12 *****
	AA	4.92 ± 0.51	4.77 ± 0.88

TA: thoracic aorta. AA: abdominal aorta. *P*-value is resulted from Student's *t* test. **P* < 0.05 compared with *Pparg*$^{+/+}$ mice.

Table S5. Sequences of primers used for real-time PCR.

Gene		Sequence	Amplicon
Mmp2	Forward	CCC CGA TGC TGA TAC TGA	152 bp
	Reverse	CTG TCC GCC AAA TAA ACC	
Mmp9	Forward	CCT GGA ACT CAC ACG ACA TCT TC	82 bp
	Reverse	TGG AAA CTC ACA CGC CAG AA	
Mmp7	Forward	GCA GGC ATT CAG AAG TTA TAT G	168 bp
	Reverse	ACC CAT CCA CAG CAC AAG	
Mmp12	Forward	CCC ACT TCG CCA AAA GGT TT	73 bp
	Reverse	CAT GAG CTC CTG CCT CAC ATC	
Ctss	Forward	GGT TGG CTA TGG GAC TCT TG	123 bp
	Reverse	GCA ATT CCG CAG TGA TTT TT	
Timp1	Forward	ATT CAA GGC TGT GGG AAA TG	183 bp
	Reverse	CTC AGA GTA CGC CAG GGA AC	
Timp2	Forward	CAC GCT TAG CAT CAC CCA	134 bp
	Reverse	TGA CCC AGT CCA TCC AGA G	
Tnf	Forward	CAT CTT CTC AAA ATT CGA GTG ACA A	175 bp
	Reverse	TGG GAG TAG ACA AGG TAC AAC CC	
Il1b	Forward	GCA ACT GTT CCT GAA CTC AAC T	89 bp
	Reverse	ATC TTT TGG GGT CCG TCA AT	
Ccl2	Forward	CCC ACT CAC CTG CTG CTA CT	164 bp
	Reverse	TCT GGA CCC ATT CCT TCT TG	
Adgre1	Forward	CTT TGG CTA TGG GCT TCC AGT C	165 bp
	Reverse	GCA AGG AGG ACA GAG TTT ATC GTG	
Eln	Forward	CTG CCA AAG CTG CCA AAT AC	99 bp
	Reverse	CTC CAG CTC CAA CAC CAT AG	
Fbln4	Forward	GGG TTA TTT GTG TCT GCC TCG	218 bp
	Reverse	TGG TAG GAG CCA GGA AGG TT	
Fbln5	Forward	TCC AAC TAC CCC ACG ATT TCA AG	229 bp
	Reverse	GGC AGT AAC CAT AGC GAC ATT C	
Fbn1	Forward	TCA TCG GAG GCT ATA GGT GTA GCT	90 bp
	Reverse	CAC TCA GGC ACT CGT TTT CAT C	
Col1a1	Forward	TCA GAG GCG AAG GCA ACA GTC	120 bp
	Reverse	GCA GGC GGG AGG TCT TGG	
Col3a1	Forward	GAC AGA TTC TGG TGC AGA GA	107 bp

	Reverse	CAT CAA CGA CAT CTT CAG GAA T	
Lox	Forward	GTC ACC AAC ATT ACC ACA GCA	186 bp
	Reverse	CAT AAC ATC CAG GAC TCA ATC C	
Loxl1	Forward	CTA TGC CTG CAC CTC TCA CA	112 bp
	Reverse	GTA GTT CCC AGG CTG CAC AT	
Eln chip	Forward	CCT CTA TGC CCT GTA CTG TAT AAG A	241 bp
	Reverse	AGG CTT TAA GGA ATG TGA AGT GTA G	
Fbln5 chip	Forward	GAT GCA CAA ATA CCC GCC AT	80 bp
	Reverse	TTG ATG AAT GCC GGA CCA TC	
Pparg	Forward	CAT AAA GTC CTT CCC GCT GA	91 bp
	Reverse	CAT GTC GTA GAT GAC AAA TGG	
rat *Eln*	Forward	CTG CAT CCA AAG CTG CTA AA	157 bp
	Reverse	CCT GCT ACT CCA CCA GGA AC	
rat *Fbln5*	Forward	GGA CCA GCC ATT CAC CAT CTT	90 bp
	Reverse	GTC GTT GCT TGC ATC TGG AA	
rat *Mmp9*	Forward	TGG ATC CCC AGA GCG TTA CT	93 bp
	Reverse	AAT AGG CCT TGT CTT GGT AGT GAA A	
human *PPARG*	Forward	GAG CCC AAG TTT GAG TTT GC	198 bp
	Reverse	CTG TGA GGA CTC AGG GTG GT	
human *ELN*	Forward	GGA GGA CTC GGA GTC GGA G	101 bp
	Reverse	CCA GCA GCA CCG TAT TTA GCT	
human *FBLN5*	Forward	GGA TCA GTG ATA ACC GCT GTA TGT	81 bp
	Reverse	TGT CCC GGT ACA AGA TGG TAA AG	

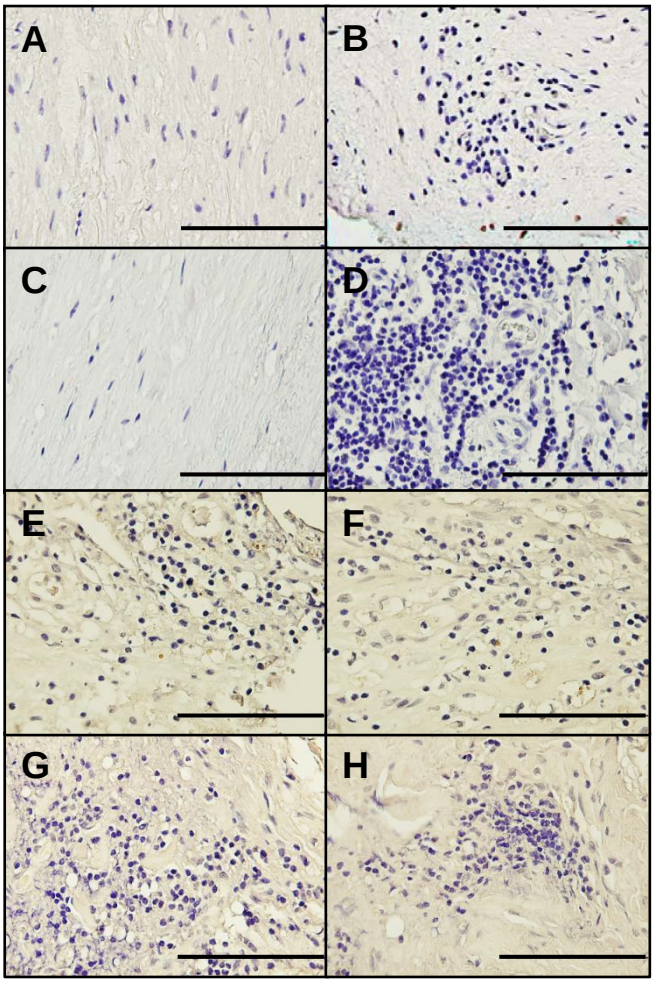

Figure S1. Negative controls of immunohistochemical staining of PPARγ in normal human abdominal aorta (**A** and **B**) and human AAA (**C**-**H**). The controls were no primary antibody (**A**-**D**), primary antibody isotype control (**E** and **F**) and no antigen retrieval (**G** and **H**) followed by incubation with secondary antibodies and detection reagents. Scale bars are 100 μm.

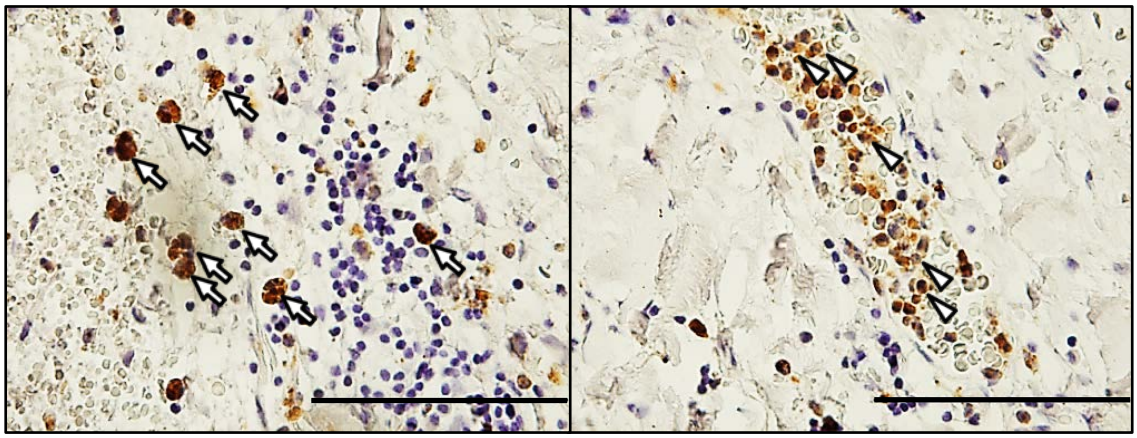

Figure S2. Immunohistochemical staining of CD68 in human AAA. A small portion of CD68-positive cells were found in the adventitia of human AAA. Some CD68-positive cells with larger cytoplasm and irregular shape are macrophages (left picture, open arrow). Other CD68-positive cells with smaller size and lightly stained nuclei are likely monocytes (right picture, open arrowhead).

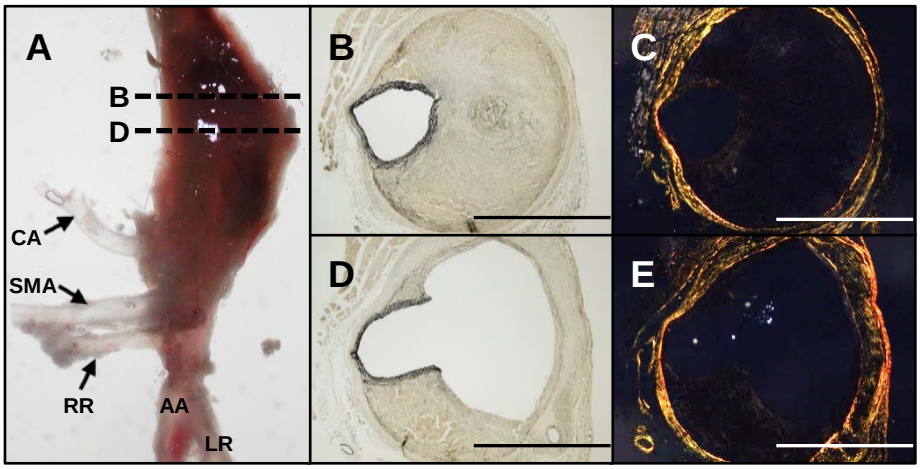

Figure S3. AngII-induced dissecting AAA in a wild-type mouse treated at 1000 ng/kg/min for 4 weeks. **A**, Gross view of aneurysm characterized by the bulge of upper portion of the suprarenal aorta. Verhoeff's stain of the section (**B**) from the upper portion shows intact tunica media and with large but organized intramural hematoma that is enclosed within relatively intact adventitia shown by the collagen in (**C**) (polarized view of PS red stained section). Section (**D**) shows torn tunica media and severely dilated false lumen that are hold by the organized hematoma and adventitia. Thickening of adventitia is highlighted by the extensive collagen synthesis in (**E**). Collagen in the organized hemostatic plugs in (**C**) and (**E**) are very limited. Scale bars are 1000 μm.

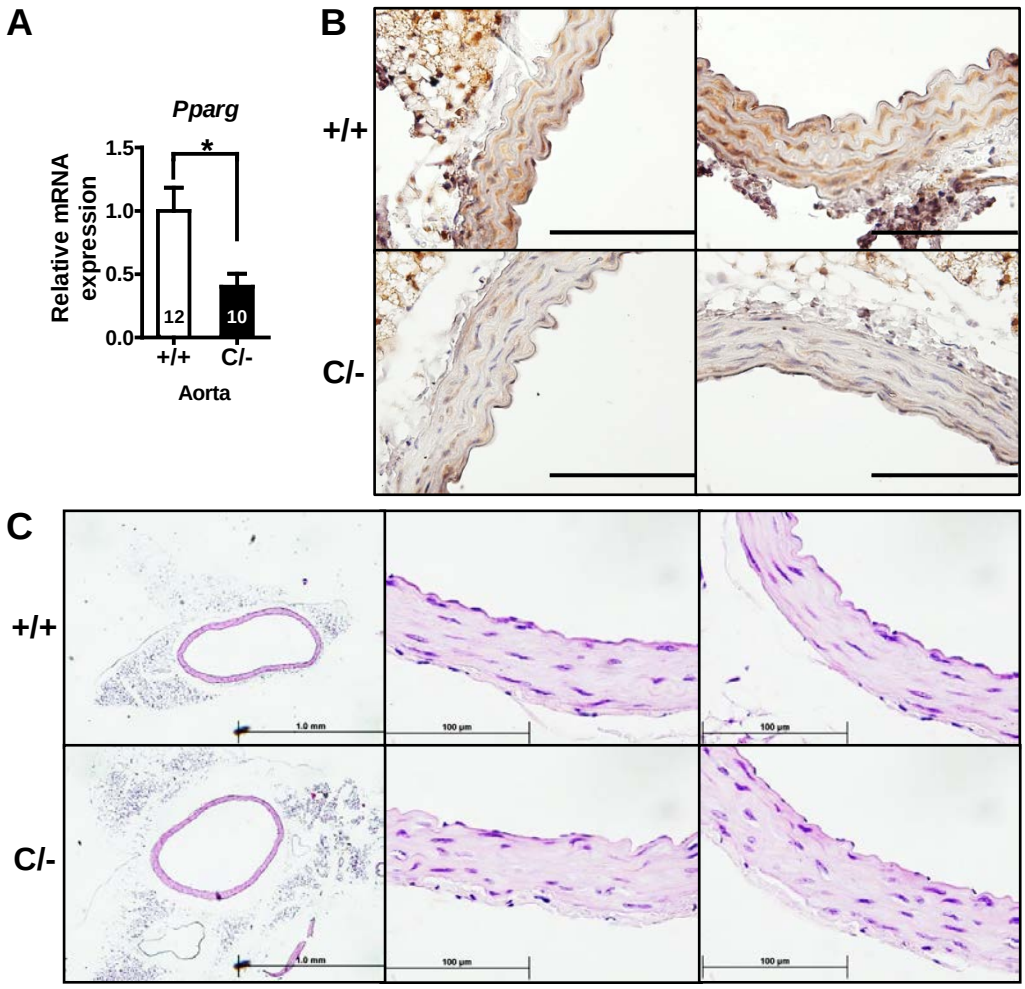

Figure S4. A, mRNA level of PPARγ in the *Pparg*$^{C/-}$ aorta is 40% normal. **P*<0.05 compared with *Pparg*$^{+/+}$ mice. **B**, Immunohistochemical staining of PPARγ in *Pparg*$^{+/+}$ and *Pparg*$^{C/-}$ aorta, confirming the reduction of PPARγ protein in the *Pparg*$^{C/-}$ aorta. Scale bars are 100 µm. **C**, H&E staining of the cross-section of aorta indicates normal vascular dimension of the *Pparg*$^{C/-}$ aorta.

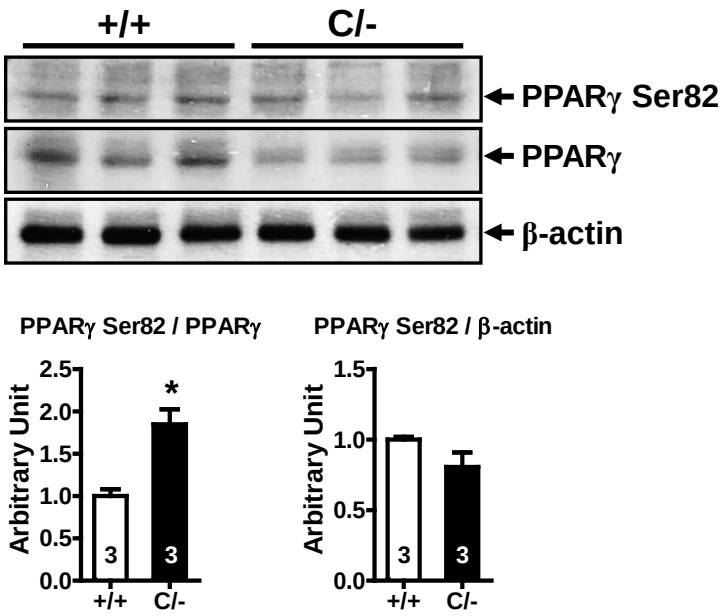

Figure S5. Ser82 phosphorylation of PPARγ in aorta was determined by immunoblotting using antibodies against P-Ser82 PPARγ and PPARγ. The relative ratio of P-Ser82 PPARγ to total PPARγ was significantly higher (1.8X, $P<0.05$) in *Pparg*$^{C/-}$ aorta than in *Pparg*$^{+/+}$ aorta, while the relative ratio of P-Ser82 PPARγ to β-actin did not differ.

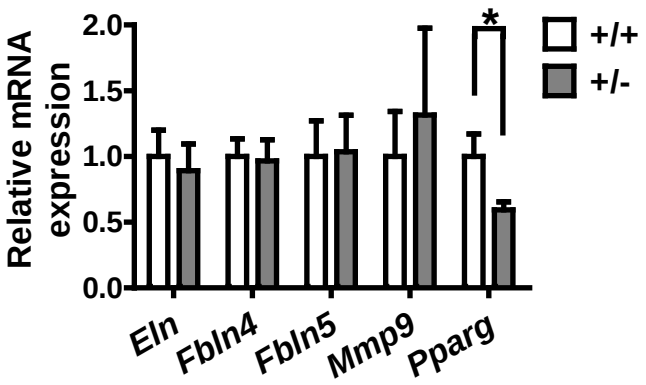

Figure S6. Expression of ECM components and MMP-9 in *Pparg*$^{+/-}$ aorta. Data are expressed relative to the mean in *Pparg*$^{+/+}$ aorta as 1.0 (+/+ = 5, +/- = 5). **P*<0.05 compared with *Pparg*$^{+/+}$ mice.

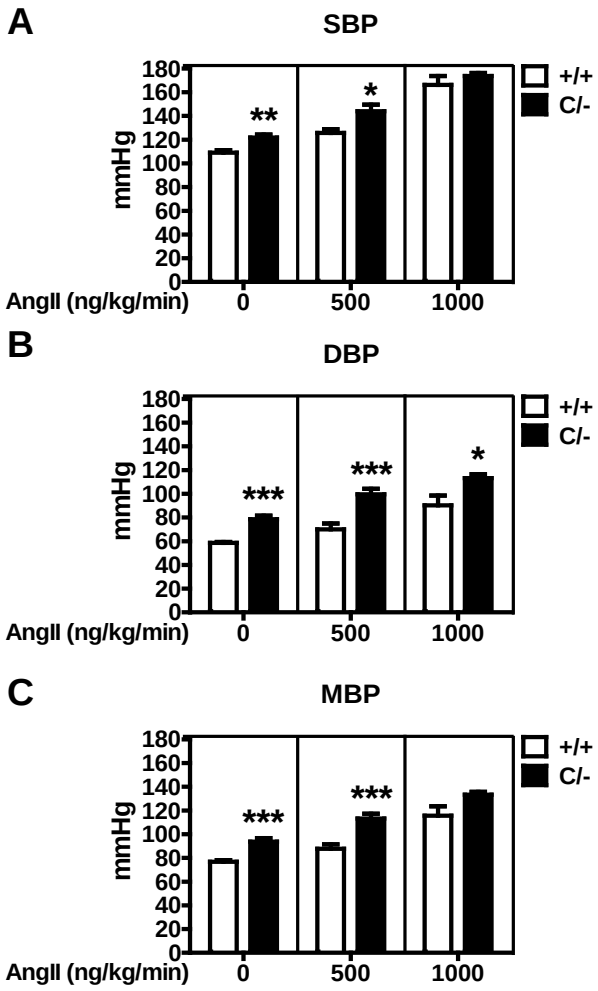

Figure S7. Tail-cuff BP measurements in mice infused with AngII (0, 500, or 1000 ng/kg/min) and fed with a western diet for 4 weeks. SBP: systolic BP. DBP: diastolic BP. MBP: mean BP. N=6, 9 and 4 in each genotype of AngII 0, 500, 1000 ng/kg/min groups, respectively.

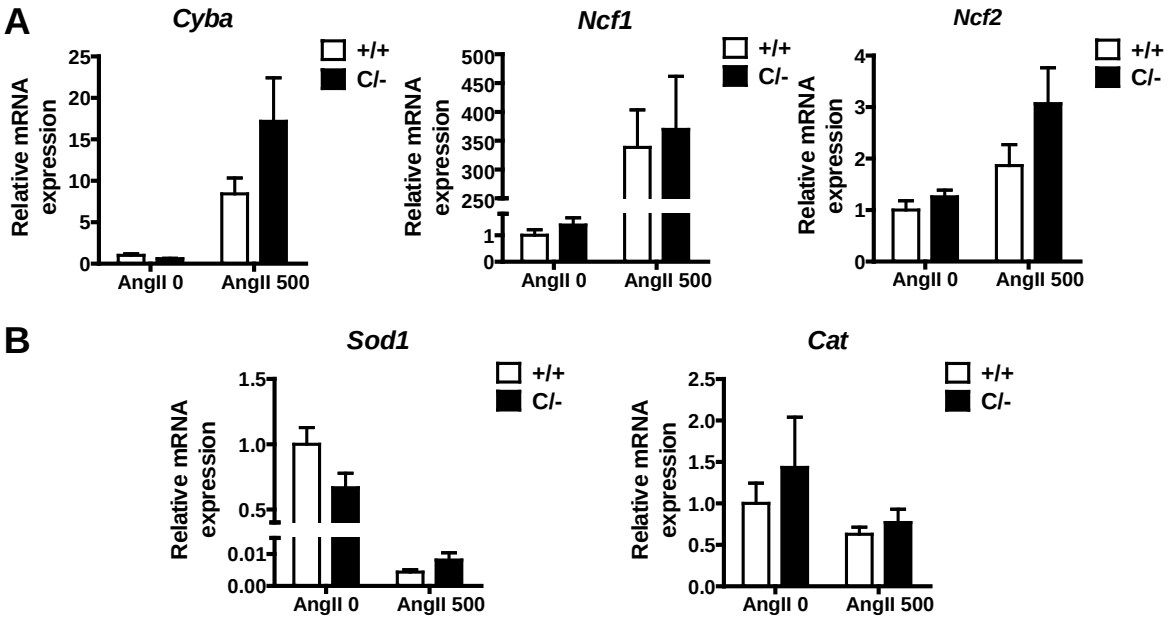

Figure S8. Expression of (**A**) pro-oxidant and (**B**) anti-oxidant enzymes in *Pparg*$^{C/-}$ and *Pparg*$^{+/+}$aorta without and with AngII (500 ng/kg/min) infusion for 4 weeks. Data are expressed relative to the mean in untreated *Pparg*$^{+/+}$ aorta as 1.0 (N=5~7 in each genotype). Two-way ANOVA analysis showed that treatment of AngII had significant effect on expression of *Cyba* (*P*<0.001), *Ncf1* (*P*<0.001), *Ncf2* (*P*=0.078), *Cat* (*P*<0.01) and *Sod1* (*P*<0.001). However, neither PPARγ genotype effect nor interaction between AngII and genotype was found in expression of all these genes.

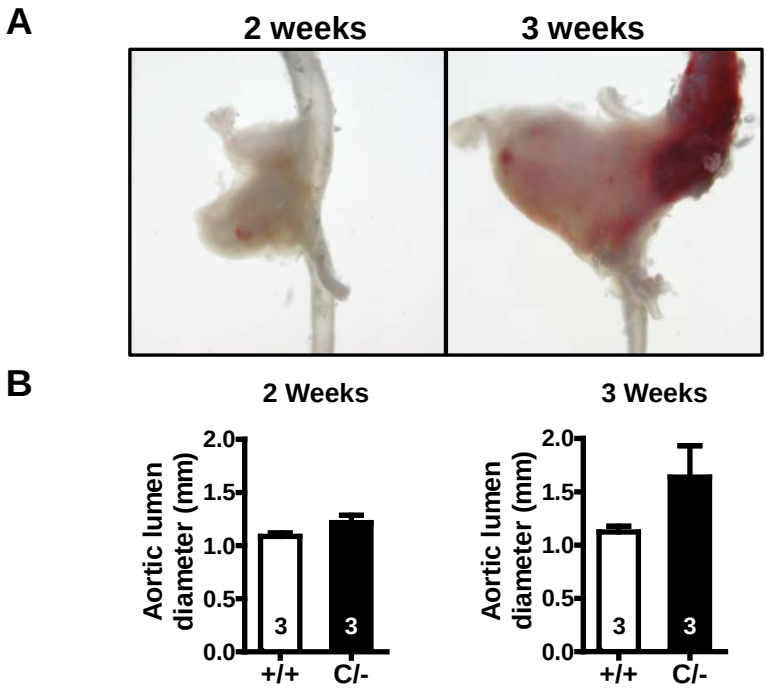

Figure S9. Time course of AAA development in AngII-infused *Pparg*$^{C/-}$ mice. **A**, Representative photographs of AAA and (**B**) suprarenal aortic lumen diameter measured by ultrasound imaging in the mice of 2 and 3 weeks post-AngII (1000 ng/kg/min) infusion. N=3 in each group.

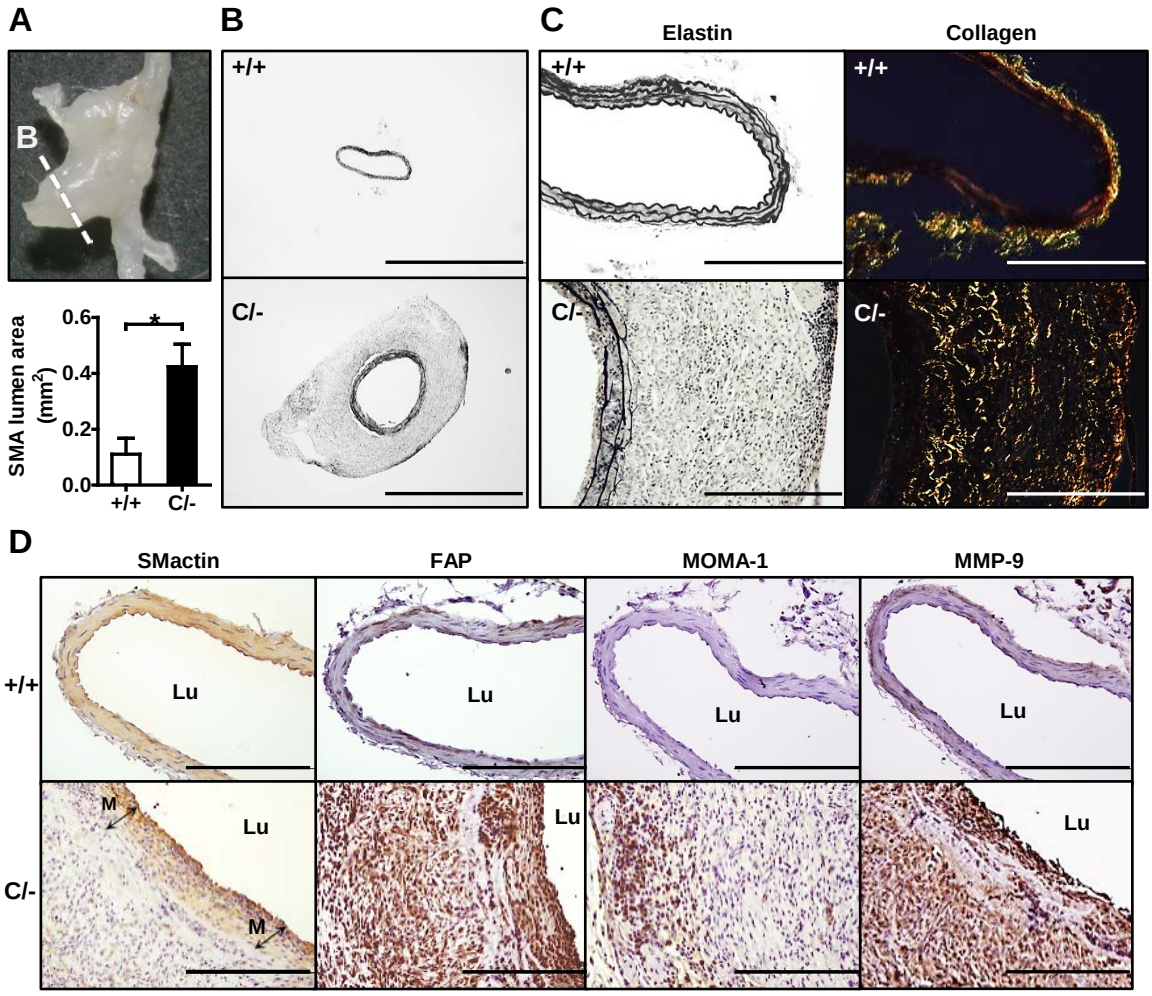

Figure S10. Histological characteristics of the AngII-infused *Pparg*$^{C/-}$ SMA aneurysm. **A** and **B**, Cross-section and quantification of SMA lumen area. **P*<0.05. **C**, Elastin and collagen (PS red) staining of SMA. **D**, Immunohistochemistry staining for smooth muscle cells (SMactin), fibroblasts (FAP), macrophages (MOMA-1) and MMP-9 in SMA. Lu: lumen. M: medial. Scale bars in (**B**) are 1000 μm and in (**C** and **D**) are 200 μm.

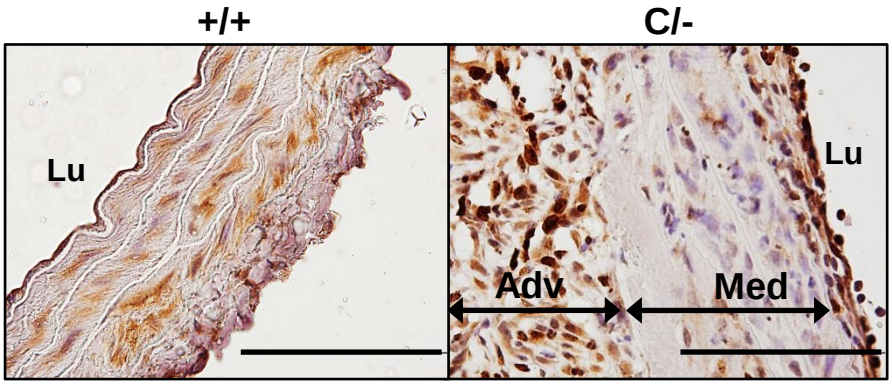

Figure S11. Immunohistochemical staining of Ki-67 in dilated *Pparg*$^{C/-}$ SMA and *Pparg*$^{+/+}$ AA after AngII (1000 ng/kg/min) infusion for 4 weeks. The dilated adventitia of *Pparg*$^{C/-}$ SMA shows a dramatic increase of Ki67-positive signal. Lu: lumen; Med: media; Adv: adventitia. Scale bars are 100 μm.

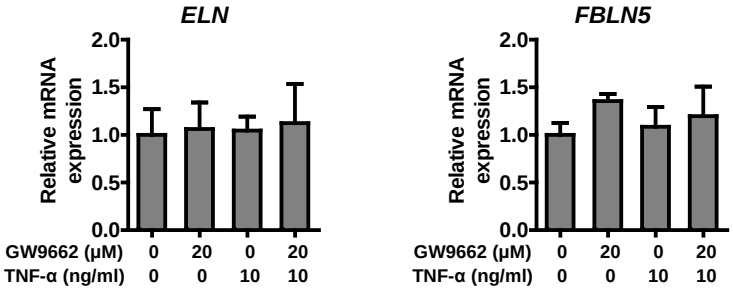

Figure S12. Expression of *ELN* and *FBLN5* after treatment with GW9662 or TNF-α in HASMCs. Data are expressed relative to the mean in untreated groups as 1.0 (N=3 in each group).